npj | Flexible Electronics

www.nature.com/npjflexelectron

ARTICLE OPEN

Check for updates

Conducting polymer tattoo electrodes in clinical electro- and magneto-encephalography

Laura M. Ferrari[1,2], Usein Ismailov[3], Jean-Michel Badier[4], Francesco Greco[1,5,6]✉ and Esma Ismailova[3]✉

Temporary tattoo electrodes are the most recent development in the field of cutaneous sensors. They have successfully demonstrated their performances in the monitoring of various electrophysiological signals on the skin. These epidermal electronic devices offer a conformal and imperceptible contact with the wearer while enabling good quality recordings over time. Evaluations of brain activity in clinical practice face multiple limitations, where such electrodes can provide realistic technological solutions and increase diagnostics efficiency. Here we present the performance of inkjet-printed conducting polymer tattoo electrodes in clinical electroencephalography and their compatibility with magnetoencephalography. The working mechanism of these dry sensors is investigated through the modeling of the skin/electrode impedance for better understanding of the biosignals transduction at this interface. Furthermore, a custom-made skin phantom platform demonstrates the feasibility of high-density recordings, which are essential in localizing neuropathological activities. These evaluations provide valuable input for the successful application of these ultrathin electronic tattoos sensors in multimodal brain monitoring and diagnosis.

npj Flexible Electronics (2020)4:4 ; https://doi.org/10.1038/s41528-020-0067-z

INTRODUCTION

Non-invasive measurement of human's biopotentials is one of the first approaches in assessment of a pathological health condition. The monitoring of such signals allows for early detection of normal and abnormal physiological functions and to prevent disease development through an effective therapy. In neurophysiology, the cortical pyramidal neurons, activated with a certain degree of coordination, generate an electrical field that is detected by means of electrodes placed on the scalp. Back in 1929, H. Berger revealed that weak electric currents generated in the brain can be non-invasively detected, despite the cerebrospinal fluid and the resistant layer of skull which protects the brain by creating a barrier for signal propagation[1]. The electroencephalographic signals are indeed the weakest among cutaneously accessible electrophysiological signals. They span from 10 up to 100 µV with a typical frequency range from 0.5 Hz to 100 Hz[2]. Following massive evolution in surface electrophysiology, electroencephalography (EEG) became one of the most popular techniques in neurophysiology due to its low invasiveness, high temporal resolution (few ms) and low-cost (in comparison with, e.g., positron emission tomography (PET) and magnetic resonance imaging (MRI)). In the last decades, the basic understanding of the mechanisms that generate spontaneous EEG activity has drastically improved. New EEG signal treatment methods emerged, starting from time-frequency analysis[3] to open source toolboxes for signal processing or sources' localization[4], enabling a better understanding of brain functions. In hospitals, EEG is primarily exercised in monitoring of alertness, coma, brain death[5], and of neurological diseases such as: Alzheimer's Disease (AD)[6] and epilepsy[7]. Brain/Neural Computer Interface (BNCI) and neurofeedback technologies became available thanks to the EEG real-time event recording and processing abilities[8]. Despite the remarkable progress in EEG fundamental understanding and in its application, the signal acquisition tools (i.e., the electrodes) did not follow similar progress. For decades, Ag/AgCl wet electrodes remained gold standard in clinical practice due to their outstanding signal-to-noise ratio (SNR)[9]. These wet electrodes establish a reliable contact with the skin by means of a conductive gel. However, the gel dries out within few hours[10], leading to electrode's performance instability over time. Known to be bulky and stiff, these electrodes cause obstructions during their placement and discomfort to the patient. The EEG patient's preparation procedure can be time-consuming[11] and it requires the presence of specifically-trained staff. The number of electrodes can vary from a few to >100, depending on the clinical request[12]. Using standard wet electrodes high-density EEG (hdEEG) recordings are often impracticable due to the gel leakage across adjacent electrodes, creating short-circuits. In order to overcome such issues, many efforts have been made towards the development of dry sensors[13]. The major limitation with basic dry electrodes, despite their slightly higher impedance[14], stands from their poor interfacing capability with the skin. This directly results in the electrode's enhanced sensitivity to movement, producing artefacts and affecting the quality of recorded signals[15]. Solutions in the form of composite materials and structures with sophisticated form factors have recently been proposed in dry electrodes designs. A "finger-shaped" electrode with polyurethane bands, enabling to access the scalp surface through the hair, have been used in EEG recordings and BCI application[16]. Self-adhesive electrodes, made of a microstructured silver microparticles-based soft composite, permitted to obtain high fidelity ECG and EEG recordings[17].

Ultrathin-film devices, which can be directly laminated on the skin, are the latest development in dry electrode technologies. These devices enable an accurate and stable contact with an extremely high mechanical conformability to the upper layer of

[1]Center for MicroBiorobotics, Istituto Italiano di Tecnologia, 56025 Pontedera, Italy. [2]The BioRobotics Institute, Scuola Superiore Sant'Anna, 56025 Pontedera, Italy. [3]Department of Bioelectronics, Ecole Nationale Supérieure des Mines de Saint Etienne, CMP-EMSE, MOC, 1354 Gardanne, France. [4]Aix Marseille Univ, INSERM, INS, Inst Neurosci Syst, Marseille, France. [5]Institute of Solid State Physics, NAWI Graz, Graz University of Technology, 8010 Graz, Austria. [6]Department of Life Science and Medical Bioscience, Waseda University, 169-8480 Tokyo, Japan. ✉email: francesco.greco@tugraz.at; ismailova@emse.fr

Published in partnership with Nanjing Tech University

npj nature partner journals

the skin[18], resulting in a seamless interface. Moreover, they can be easily designed and manufactured for large-area coverage applications[19]. Various strategies are emerging for obtaining skin-compliant electrodes based on ultrathin polymer films with conductive materials, like metals and graphene[20]. The temporary tattoo electrodes (TTEs) have been developed using organic materials[21]. These are conducting polymer-based dry skin-contact sensors made of poly(3,4-ethylenedioxythiophene): polystyrene sulfonate (PEDOT:PSS), deposited by spin-coating or inkjet printing, on top of a commercially available temporary tattoo paper. Thanks to their sub-μm thickness and softness, TTEs are capable to conformably adhere to the skin creating an imperceptible contact between the human body and the electronics. Multiple examples have demonstrated TTEs' successful use in electromyography (EMG) and electrocardiography (ECG). Their performance has not only been proved through their mechanical robustness but also via their long-term electrical stability to monitor biosignals. The latter was evaluated using skin-contact impedance measurements over up to 48 h together with electrophysiological recordings. Additionally, TTEs are perforable, since hair can grow through them, without impairing the quality of recorded signals[22]. It is well known that hair growth is an important issue in cutaneous technologies. For instance, hair growth causes sensor displacement and signal loss in clinical long-term electrophysiology. Therefore, TTEs combine necessary properties as long-term monitoring tools, particularly sought in EEG assessments.

In clinical practice, EEG recordings are frequently coupled with magnetoencephalography (MEG). While EEG records electric field changes in the brain, MEG senses variations in the magnetic field induced by modifications of the electric field generated by the same population of neurons. Simultaneous EEG/MEG recordings are essential in understanding of dynamic cognitive processes, owing to their high temporal resolution[23]. As the EEG electrodes are prone to interfere with the MEG sensors, special requirements and precautions must be considered. Certain metallic electrodes can indeed produce artefacts obscuring the detection of the magnetic field (further detailed below). The metal-free EEG electrodes in such experimental setups promise to offer a minimal magnetic signal perturbation.

Here we investigate TTEs' performance in recordings of low amplitude EEG signals and their potential to integrate a standard clinical evaluation protocol for brain health assessment. In order to understand how efficiently TTEs transduce the biosignals we investigate their contact impedance, looking in detail into the equivalent circuit model of Ag/AgCl and tattoo electrodes. Then, we carry out three experimental evaluations usually adopted for epilepsy: spontaneous brain activity recordings (alpha waves monitoring), artificially induced activity (auditory evoked potential, (AEP)) detection, and simultaneous MEG/EEG recordings. In MEG, the high number of sensors allows restitution of the brain activity mapping with a great spatial resolution. Using a skin-mimicking phantom, we explore the feasibility of hdEEG with tattoo electrodes. The compatibility of TTEs with MEG and their high-density recording capability are aimed to offer advanced tools for neurodegenerative disease diagnostics with high tempo-spatial resolution[12].

Temporary tattoos are an attractive platform for skin-worn devices, offering a unique opportunity to develop body-compliant sensors which are continuously in contact with the skin[24]. While the broader concept of epidermal electronic devices was originally launched by Rogers' group[25], tattoo-based electrochemical sensors have been developed for sweat sensing by Wang's group[26]. In the last decade, the field is expanding significantly due to its potential application in wearable electronics[27]. At present, the physical mismatch at the electronic–skin interface is a well-known issue in advancing the field of the next-generation of wearable devices[28]. Two key aspects are involved in the development of skin-conformable interfaces: the low thickness (in the nm–μm range)[29,30] and the elastic modulus, comparable with the skin (0.1–1000 KPa[31]). Commercially available temporary tattoo papers have a layered structure (Fig. 1a) that comprises a sub-μm—μm thick polymer decal film (whose composition and thickness varies among different types and providers), releasable from its paper support by wetting, due to the dissolution of the water-soluble sacrificial layer. This tattoo film can be then directly laminated onto any surface (typically skin) ensuring its complete conformability. This film is imperceptible for the user, as in the case of a temporary fantasy tattoo for children.

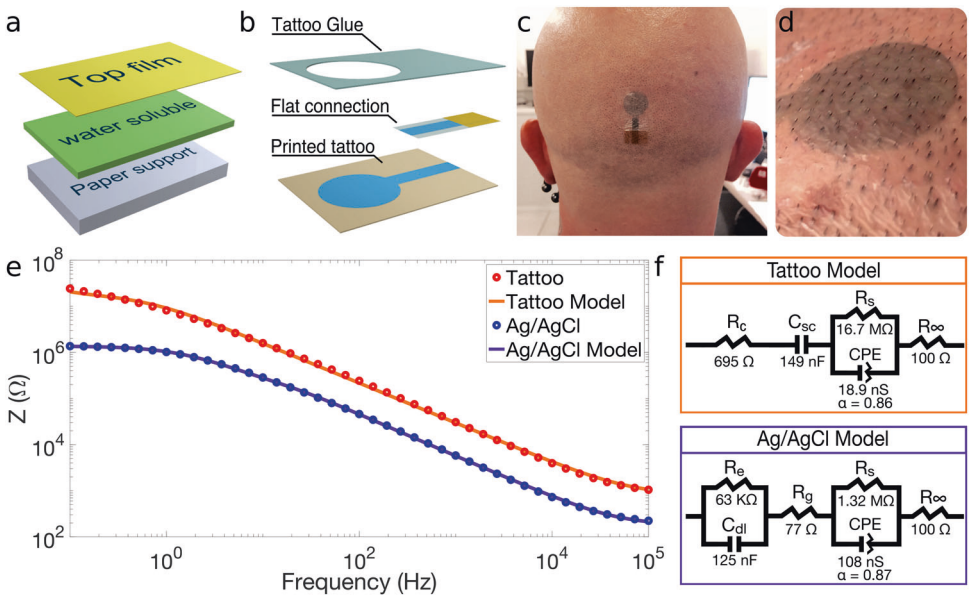

Fig. 1 Temporary tattoo electrodes (TTEs) for EEG. a The layered structure of the temporary tattoo paper permits the release of the top film on which electrodes are fabricated. **b** Expanded view of an all-polymer printed TTE. **c** A TTE released on the scalp, in Oz position. **d** Close-in view of a TTE released on the scalp after 12 h from application. **e** Impedance recordings on the forearm using TTE and Ag/AgCl electrodes. The data were fitted with models depicted on the right. Details on the model are given in the main text.

The materials and the fabrication protocols adopted here for the development of the tattoo electrodes have been rethought, with respect to our previous publication[22], fitting stringent requirements related to the EEG and MEG evaluations. The electrodes and external connector design are made to achieve high quality and low noise recordings. A polyurethane/allyl resin-based decal transfer film with a 1.5 µm thickness. This allows for improved mechanical stability of tattoo electrodes on the skin, with respect to the previously reported 500 nm thick ethyl cellulose[22], while maintaining their unperceivability on the skin. Details are given in Methods section and the schematics of the tattoo electrodes layers is provided in Supplementary Fig. 1. The electrodes sensing area and interconnections are made of PEDOT:PSS due to its low mechanical stiffness, compatible with tattoo releasable polymer film as well as with the skin mechanics, and potential MEG compatibility. It is also the most popular conducting polymer in bioelectronic applications[32,33]. PEDOT:PSS is a metal-free material that can be fabricated by low temperature processing[34] with large-scale integration capability at low-cost. Numerous implementations of this polymer in recordings of electrophysiological signals have been successful demonstrated[35]. Particularly, the PEDOT:PSS-coating of metallic electrodes have enhanced SNR in EEG recordings as it lowers the interface impedance of the electrode by increasing its contact surface with the skin[36]. As a solution processable material its deposition can be achieved in multiple ways. Inkjet printing of TTEs has two advantages over screen printing, namely: minimal material waste during the production process[37] and low ink viscosity, thus resulting in an ultrathin layer deposition. A single printed layer of PEDOT:PSS has a thickness of 240 ± 30 nm, while a 2-layers has a thickness of 360 ± 30 nm. Two consecutively inkjet-printed PEDOT:PSS layers reduce the overall electrical resistance while preserving their mechanical conformability of the TTE[22]. A more detailed study on the electrode performance as a function of the number of PEDOT:PSS- printed layers is included in Supplementary Fig. 1.

The main and most challenging issue in thin-film epidermal electronics is the interconnection of soft, almost imperceptible devices, with hard electronics. Indeed, the soft/rigid interface can easily rupture during electrodes mounting or the participant movement. To this aim, a specifically designed external connection made of a thin (1.3 µm) and flexible polyethylene naphthalate (PEN) sheet and a dedicated plastic clip was developed, improving the robustness of the connection and in turn resulting in reliable recording of the brain biopotentials. This metal-free flat contact reduces the electromagnetic noise and the interference with other equipment, as especially required in MEG. A monolithically assembled sensor and contact lead, shown in Fig. 1b, facilitate handling during placement on the scalp, which is done in a single step. An example of TTE laminated on the human scalp is shown in Fig. 1c, d.

RESULTS AND DISCUSSION

Impedance evaluation of TTEs working principle

In EEG, the evaluation of the contact impedance is taken as a reference point for electrode's characterization, prior to recordings. As a general rule, a high impedance onset, when using standard gel-assisted Ag/AgCl electrodes, leads to a low SNR[38]. In order to investigate the TTE/skin interface we elaborate a model based on impedance evaluations and compare them with those obtained with medical grade Ag/AgCl electrodes (Fig. 1e, f). Two analytical models are developed, one for the wet Ag/AgCl electrodes and one for the dry TTEs (Fig. 1f). In both cases, the skin component is represented with a traditional Cole model[39] (right part of the model), a resistor (Rs) in parallel with a constant phase element (CPE), in series with another resistor (R_∞). The Rs and the CPE model the stratum corneum (SC), the outermost layer of the epidermis, which plays a major role in the skin impedance[40]. The Rs represents the SC conductivity while the CPE embodies the SC capacitance. The CPE describes a capacitor with an inhomogeneous surface having an impedance $Z_{CPE} = 1/Y_0(j\omega)^{\alpha}$ [41], where Y_0 is the admittance (S), j is the imaginary unit, ω is the angular frequency of the electrical signal, while α is a dimensionless constant ranging between 0 and 1; when $\alpha = 1$ the CPE is an ideal capacitor. The R_∞ is the resistivity of the epidermal tissue underneath the SC, and it is the only element that is the same for wet and dry electrodes. The R_∞ is fixed at 100 Ω as per the literature[42]. Two different models are adopted regarding the skin-contact impedance (left part of the model). Ag/AgCl electrode is described with the state of the art model: a parallel network of a capacitor (C_{dl}) and a resistor (R_e), followed by a resistor (R_g) in series[43]. The Cdl is the double layer capacitor at the metal/ionic gel interface, while the R_e represents the charge transfer due to the faradaic current at the same interface. The R_g is the gel resistivity. Traditional dry electrodes usually tends to establish a wet interface with the skin due to the perspiration within a few hours[14]. Thus, their behavior describes the one of a wet electrode, where the sweat layer replaces the gel function. However, TTEs' impedance follows a capacitive trend and we do not observe the formation of sweat with time. This is confirmed by the absence of a change in the impedance shape, resembling the one of wet electrodes, as it happens in dry electrodes. Indeed, differently from traditional dry electrodes, TTEs are completely conformable and follow intimately the skin surface relief[22]. In order to account for these differences we develop a dedicated model ("Tattoo model" in Fig. 1f). The description of the TTEs impedance is based on the hypothesis where such electrodes transduce the signal as a capacitor (C_{sc}), having the first layer of the SC as a dielectric[44]. The SC consists of a layered structure of keratinized cells surrounded by their extracellular matrix, and it has a thickness of a few µm[45]. The capacitive element is followed by a resistor (R_c) in series, representing the resistivity of the electrode and the connection. The two impedance spectra (Fig. 1e) show similar typical behavior, with the impedance modulus decreasing as the frequency increases. A remarkable difference is however observed in the low frequency range ($f < 10$ Hz), mostly interesting for the low frequency content of EEG signals, with a $Z = 2.8 \times 10^5$ for Ag/AgCl electrode and $Z = 1.6 \times 10^6$ TTE at 10 Hz. This difference is mainly due to skin hydration. The SC conductivity indeed changes with water content[46]. According to this, the calculated R_s value for the Ag/AgCl electrode model is 1.32 MΩ cm^2, while for TTE it is 16.7 MΩ cm^2. Also the CPEs show the same trend, with skin hydration playing a major role[47,48]. Here, the calculated pseudo-capacitance of dry TTE is 5.4 times lower than the one of Ag/AgCl electrode, (15 nF cm^2 for TTE and 81 nF cm^2 for Ag/AgCl electrode), and is in complete agreement with previously reported data (20–60 nF cm^2)[46]. It is remarkable that TTEs interface the skin in a completely different manner than wet and dry electrodes. Regardless of their impedance characteristics, such ultrathin electrodes allow for a high-quality signal transduction of biopotentials accessible from the skin. This statement is supported by the electrophysiological recordings and their analysis (i.e., SNR), presented in the following section.

Alpha waves recordings

Recording of a well-defined electrophysiological activity serves as a relevant validation of TTEs function. The brain activity changes when the subject passes from a state of alertness to relaxation. In this case the alpha waves, the most studied rhythm of the brain, arise prominently from the occipital lobe. Alpha waves appear in an 8–12 Hz frequency range with a typical amplitude of 50 µV (peak-to-peak)[2]. Such spontaneous brain activity is detected by TTEs (Fig. 2), from the Cz–Oz derivation, identified according to the 10–20 international system (Fig. 2a). In the time-frequency plot

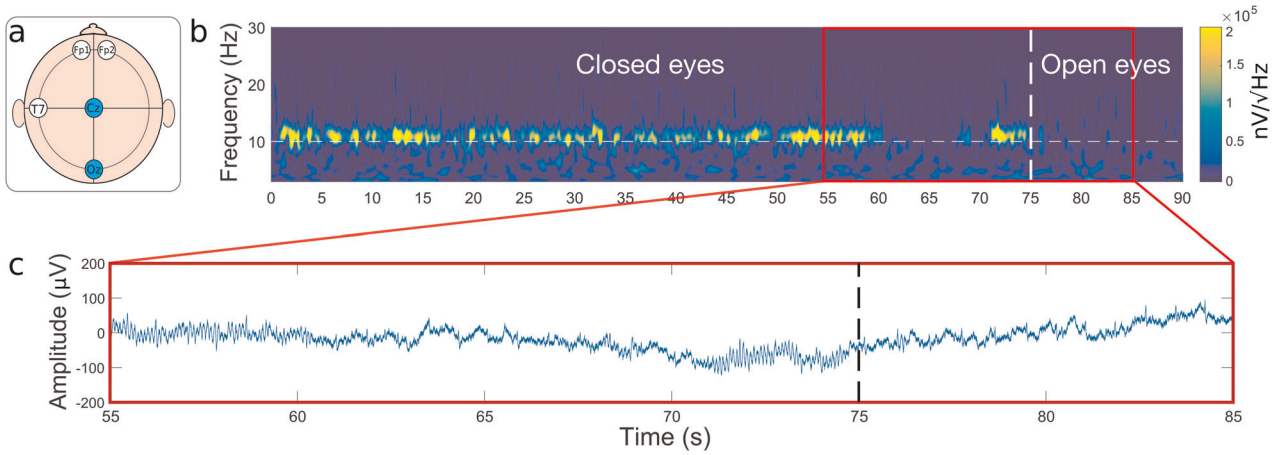

Fig. 2 Electroencephalography recording with TTEs on human scalp. a Schematic mapping of the electrodes localization on the head, according to the 10–20 international system, with highlighted Cz–Oz derivation adopted for the recordings of spontaneous brain activity. **b** Time–frequency plot with visible Alpha activity at 10 Hz. Alpha waves momentarily disappeared for 10 s, as the subject heard an environmental noise while still in relaxing phase. At 75 s, the participant was directly asked to open his eyes (distinct by vertical white dotted line). **c** The amplitude-time plot near 75 s. The EEG recording shows alpha waves oscillations from 55 to 60 s and from 71 to 75 s, representing wakeful relaxation state.

(Fig. 2b), the alpha rhythms are centered around 10 Hz during one minute of relaxation with closed eyes. They usually disappear when the participant opens his eyes. At the 60–70 s interval we can notice that the alpha activity is vanished some seconds before the explicit request to open the eyes (at 75 s, Fig. 2b, c). This provided a meaningful validation of the electrophysiological nature of the performed recordings. The amplitude of the EEG signals is shown in the zoomed view from 55 to 85 s time interval in Fig. 2c. The average peak-to-peak amplitude of the alpha waves averaged over 1 s recording was 25 ± 14 μV.

The comparison in recordings with medical grade Ag/AgCl electrodes is also investigated, among the T7-Oz derivation. Figure 3a, b shows the time–frequency plots of alpha waves recorded with tattoo and medical electrodes. The power spectral density (PSD) is extracted to quantify the signal power distribution over a 3–40 Hz frequency range (Fig. 3c). The maximum peak signal magnitude, around 40 dB, for both types of electrodes is located at 10–11 Hz (the typical frequency of the alpha waves) and, in agreement with results obtained with other flexible and dry electrodes[49]. Notably, both TTEs and Ag/AgCl electrodes are able to catch slow waves (0.5–4.5 Hz), whose recording is very challenging and which are fundamental in sleep studies. A typical 1/*f* shape behavior can be observed in both recordings. At around 20 Hz the TTEs' signal magnitude is significantly higher than the one of the Ag/AgCl. The electronics 1/*f* noise, known as Flicker noise and related to the defects in semiconductors[50], can be considered equal in both recordings. However, in EEG much importance is given to the 1/*f* electrophysiological noise, known also as a neural noise. This signal has a biological meaning and thus should be carefully processed. The neural noise results from a temporal correlation within the neurons activity[51] and can be assigned to different physiological states, such as ageing[52]. The stronger magnitude in TTEs recordings suggests that these electrodes are more sensitive. A higher SNR is found using TTEs in evoked potential recordings, discussed hereafter, further supporting this statement.

Concerning the possible integration of tattoo electrodes in clinical evaluations, EEG recordings have been also performed on a medical-grade equipment in a hospital evaluation room. No special units such as a faraday cage or the impedance matching components are used to connect tattoo electrodes to the recording unit. TTEs are able to record well-defined alpha waves during the 2 min session, with 30–50 μV peak-to-peak amplitude (see Supplementary Fig. 2). The signal is comparable with those recorded by standard Ag/AgCl electrodes.

Auditory evoked potential (AEP) recordings

Evoked potential recordings represent a powerful tool for an objective assessment of cognitive statuses such as attention, memory, and language[53]. Evoked potentials are time-locked task-oriented events, induced by an external stimulus, with an amplitude lower than 10 μV. In order to distinguish such small signals from regular brain activity, the stimulus is averaged over hundreds of times (550 in our case) which leads to the generation of a well-defined pattern. Figure 3e shows a comparison of an AEP, induced by bursts of brief sinusoidal auditory stimuli, acquired with both TTEs and Ag/AgCl from T7-Cz and sT7-sCz derivations, respectively. Both type of electrodes detect a characteristic waveform of a neurological response, the N100. This takes place between 80 and 120 ms after the stimulus, and its amplitude is strongly dependent on the rise time of the stimulus onset[54]. We then calculate the SNR, defined as the ratio between the signal maximum peak-to-peak amplitude after the stimulus is delivered, and the noise maximum peak-to-peak amplitude before the stimulus. A higher SNR, 4.07 (absolute value), is obtained with TTEs, in comparison with 3.36 for the Ag/AgCl electrodes. Owing to the high signal quality recording, together with an easy electrode placement and long-term recording capability, TTEs show a good potential for their further implementation in clinical cognitive brain assessments, long-term neuromonitoring at home and application in BCI for disabled persons.

MEG compatibility

Simultaneous EEG/MEG recordings are essential in focal epilepsy diagnostics, where seizure localization is required for defining its clinical strategy of treatment[55]. The compatibility of the EEG setup with the MEG instrumentation is a key concern in the clinical brain evaluation. Beside the adoption of low noise amplifiers, ferromagnetic materials, particularly in electrodes, are forbidden in order to avoid the generation of magnetic artefacts[56,57]. Among metals, the copper, even if diamagnetic in principle, is excluded since the naturally grown ferromagnetic copper oxide. Furthermore, the bulky geometry of EEG electrodes is also a limiting factor[55]. Their vertical profiles have to be minimized to allow an efficient coupling with the MEG sensor. Therefore, the metal-free ultrathin EEG sensors are highly attractive from the point of view

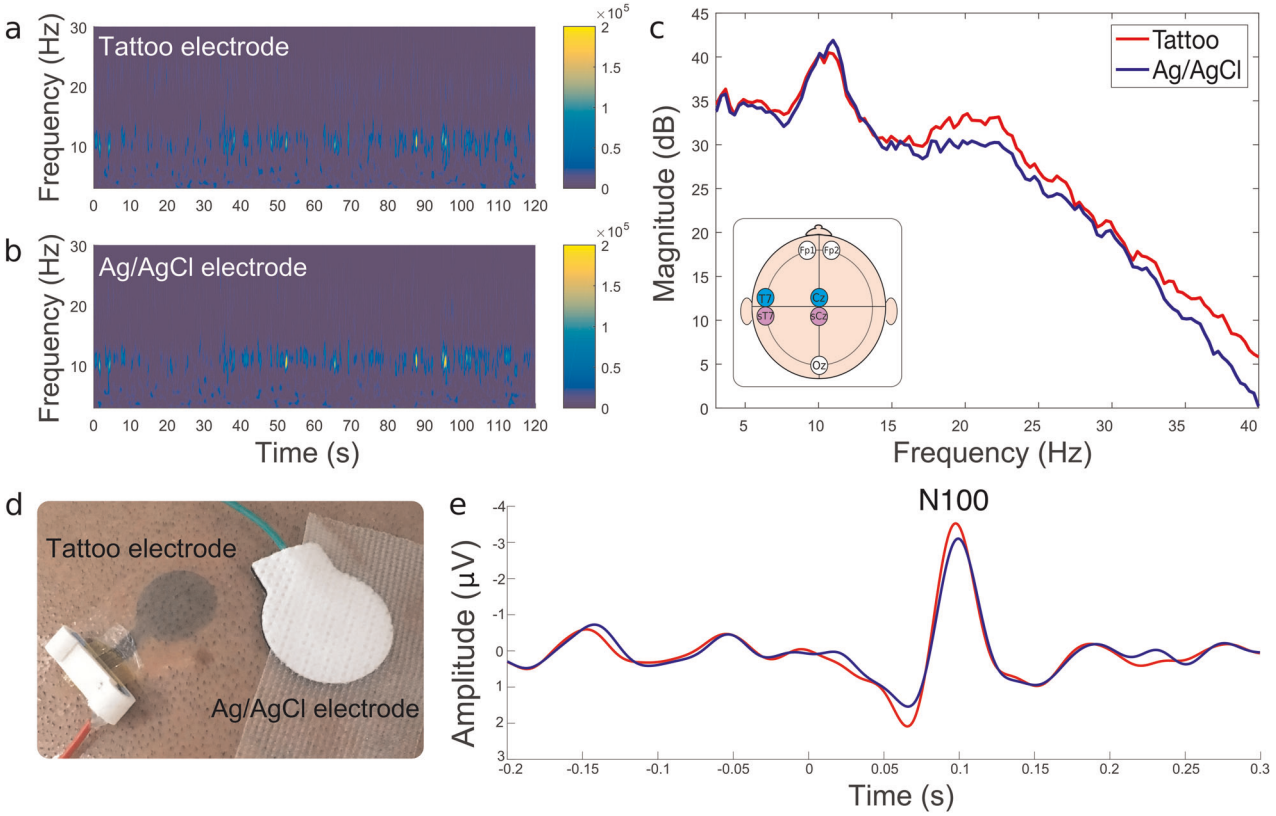

Fig. 3 Comparison of recording performances between TTEs and Ag/AgCl electrodes. a, **b** Time-frequency plot of alpha wave recordings, with visible 10 Hz activity obtained with tattoo (**a**) and AgAgCl (**b**) electrodes. **c** Superimposed PSD (dB) during alpha wave recordings from TTEs—in red, and Ag/AgCl electrodes—in blue. The insert at the bottom left shows the electrodes placement with used derivation (Tz–Cz, in light blue for the TTE, and sT7-sCz for the Ag/AgCl electrodes in light violet). **d** Picture of two electrodes in Cz position on the head of the participant. **e** Auditory Evoked Potential recorded with both TTEs (red) and Ag/AgCl electrodes (blue), with N100- an auditory evoked potential component.

of electro-magnetic neutrality and their physical compactness. To this aim, fully polymeric tattoos are designed to enhance the compatibility of EEG electrodes with MEG. They are then laminated on the participant's head, which is placed under the MEG apparatus (Fig. 4). The MEG evaluations with segmented topographical brain waves representation recorded with TTEs in place are shown in Fig. 4a, b. A neural activity is clearly visible at different frequencies without any high-density magnetic flux appearance in the EEG electrode proximity. The EEG and MEG recordings are also performed simultaneously in this study (Fig. 4c). In both recordings, alpha waves are well visible from the Oz location in the EEG and from the MEG sensor, located in the left occipital region. Due to the different physical principles of each methodology, the two recordings do not present the same topography and they are considered as complementary. To the best of our knowledge, this is the first demonstration of dry organic electronic electrodes performance in joint EEG/MEG evaluations.

Phantom platform for high-density recordings evaluation

A non-invasive localization of the intra-cerebral electric sources in the brain can be performed through hdEEG recordings. The maximum number of electrodes using medical standard Ag/AgCl electrodes is typically restrained to 32, at most 64, due to the possible electrodes crosstalk[58]. Therefore, the scalp surface recordings do not directly indicate the location of the triggered neurons in the brain. Many different source configurations can indeed generate the same distribution of potentials and magnetic fields while propagating to the surface of the scalp[59]. Different computational techniques exist, such as EEG source imaging (ESI), to estimate the location of an initiated neural activity[60]. However, theoretical and experimental studies demonstrated that a minimum of 100 electrodes is needed to properly sample the electric field from the head surface of an adult[61]. For this reason, the development of technologies that allow to increase the number of recording electrodes would be an actual improvement in clinical source localization. In order to demonstrate the capability of TTEs in resolving signal sources we developed a phantom setup, mimicking the skin interface and integrating a stimulation-recording unit, used as a well-controlled test bench (Fig. 5). A common problem in testing any health-monitoring skin-mounted device, is the large impedance variation inter and intra-subjects (due to natural factors as gender, age, hydration, stress). The use of a controlled medium, with a set impedance, is therefore a key element to intrinsically characterize the electrodes. It also offers an opportunity to combine multiple requirements, such as to apply a defined signal to the studied electrodes through an electrically resistive interface.

We therefore sought for a phantom setup which could approximate as much as possible the typical impedance of the skin. The phantom is composed of an agarose gel swollen with a saline solution. Its ionic content defines the phantom conductivity, optimized to match the typical value observed on scalp, 0.34 S/m[62]. Different types of electrodes can be placed on top of the gel, while stimulation is initiated from the bottom. The stimulation unit is made of four electrodes delivering two types of spaced input signal forms simultaneously (Fig. 5a): a peak (left electrodes) and a square wave (right electrodes). Figure 5b schematically shows the working setup. An output signal is recorded with four TTEs and two Ag/AgCl

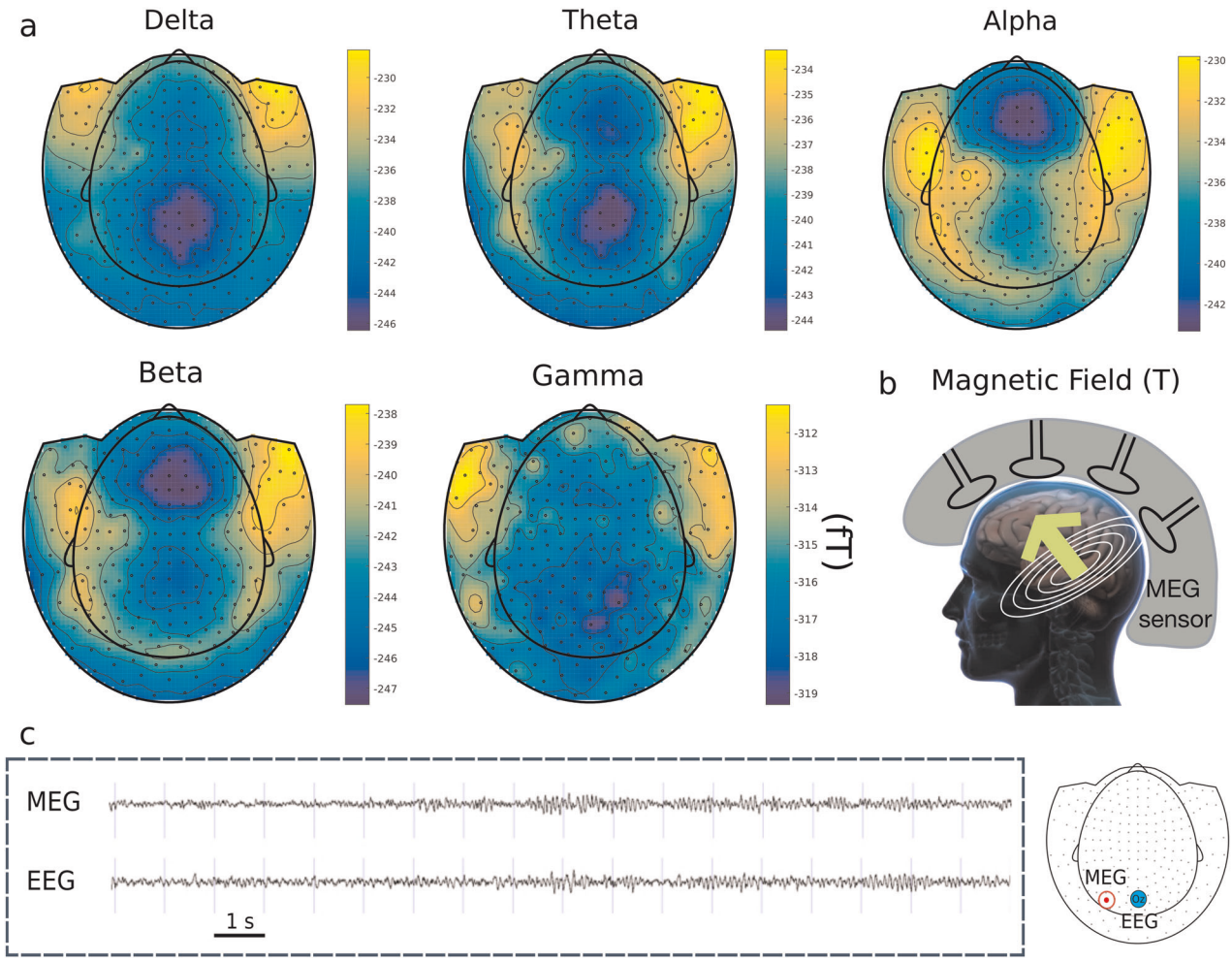

Fig. 4 Compatibility of TTE with magnetoencephalography (MEG). a MEG recording with TTEs on the head of the subject, depicted onto a head map. The signal is shown fractioned in the most known five frequency windows: Delta (2–4 Hz), Theta (4–8 Hz), Alpha (8–12 Hz), Beta (12–30 Hz), Gamma (30–120 Hz). **b** Exemplification of MEG sensors coupling with the human head. **c** Simultaneous MEG and EEG recordings with TTEs. On the right, the schematic representation of MEG sensor (right posterior location) and TTE (Oz location) from which two recoded signals are acquired. In both modalities, the presence of alpha waves appears after 8 s.

electrodes placed on the phantom top surface. The inter-electrode distance between Ag/AgCl electrodes is fixed at 33 mm corresponding to a 64 electrodes configuration on the head[63]. On the other hand, TTEs are placed at 20 mm center-to-center distance in order to double the density of electrodes with respect to the Ag/AgCl case.

In our experiments, the output signals are acquired in bipolar mode, from the pair of Ag/AgCl electrodes and from the two pairs of TTEs. The recorded signals (Fig. 5c) show that with two pairs of TTEs it is possible to identify the input source by analyzing the amplitude variation of the recorded signals. Indeed, it is clearly visible how the right couple of TTEs (the red signal in Fig. 5c), that is located near the peak signal source, are able to detect higher intensity signal. The amplitude of the peak recorded with the right TTEs is of the same order of magnitude than with the Ag/AgCl (the blue signal in Fig. 5c). The peak amplitude is equal to 7.6 mV in the left TTEs, 13.9 mV in the right TTEs, and 25 mV in the Ag/AgCl electrodes. The higher amplitude in Ag/AgCl recordings is explained by the bigger surface coverage with these electrodes, which includes the location of all four stimulating electrodes underneath. Notably, the sensitivity to the square wave stimulation of the left pair of TTEs is well apparent. Indeed, the left pair of TTEs (the purple signal in Fig. 5c), which is closer to the square wave signal, showed a more marked response to this wave, when it propagated through the RC module of the phantom. Ag/AgCl electrodes do not observe such precision in signal definition. This example demonstrates that by increasing the density of electrodes it is possible to reach higher resolution recordings and to perform a more accurate signal localization in bipolar recordings.

Additionally, unipolar signal recordings, using the same phantom platform with the same electrodes configuration, are shown in Supplementary Fig. 3. Signals discrimination is possible by looking at their amplitude in a single electrode recording. The recorded signals from the two TTEs and the Ag/AgCl electrode facing the peak wave (5 Hz square waveform) stimulation have an amplitude equal to 20 mV for the left TTE (closest to the source signal electrode), 6.1 mV for the right TTE and 14 mV for the Ag/AgCl electrode. The difference in amplitude between two adjacent TTEs' recordings is therefore 13.9 mV, which corresponds to 70% of the signal. Of course, in the physiological source localization, the body complexity does not allow such a straight dependency and sophisticated methods are required to extract the origin of propagating signals. However, these experiments show that TTEs are an enabling technology to accomplish hdEEG, used to perform non-invasive surface EEG source localization.

The physical form aspect of TTEs allows to surpass the current number of electrodes used in clinical EEG, thus allowing to resolve neuronal activity source localization. The possibility to better define specific cortical areas responsible for pathological brain

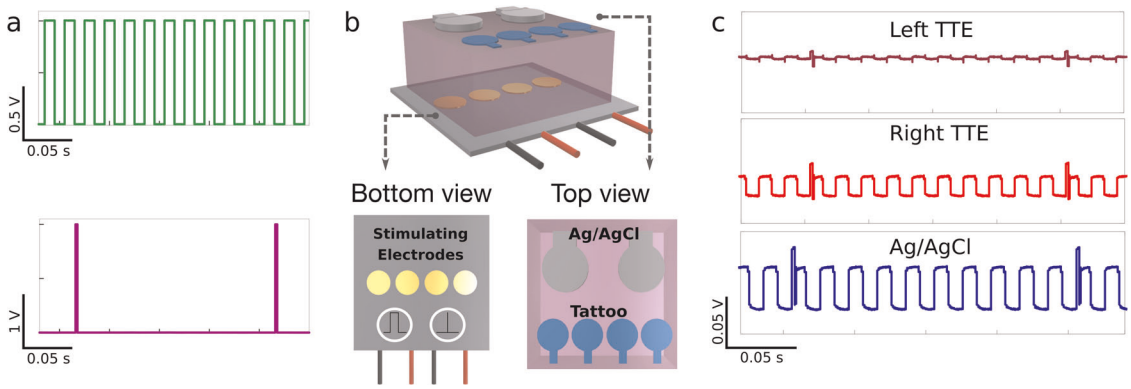

Fig. 5 High-density EEG recording through the phantom experimental set-up. a Input signals from the bottom stimulating electrodes: the 50 Hz square wave is sent at the left couple of electrodes (top) and the 5 Hz square wave sent at the right couple of electrodes (bottom). **b** Rendering of the phantom with recording electrodes positioned on top. Bottom view of the input electrodes dedicated to initiate bipolar inputs. Top view of the phantom with Ag/AgCl electrodes and TTEs. **c** The recorded output signals from the phantom. From the top: the signal from the left couple of TTEs; the signal from the right pair of TTEs; the signal from the Ag/AgCl electrodes.

activity would be of great impact in the surgical evaluation of epileptic patients.

METHODS

Materials

PEDOT:PSS aqueous dispersion (Clevios PJet 700 by Heraeus) is used as an ink to print the electrodes and the flat connections. Commercially available temporary transfer tattoo paper kit (Silhouette America, Inc, US) is adopted for the fabrication of the electrodes. The tattoo kit is composed of two sheets: the decal transfer paper and the glue sheet employed as unconventional substrate and passivation layer, respectively. The decal paper is made up of four layers: a paper carrier, a polyvinyl alcohol (PVA) water soluble layer, a releasable layer made up of a mixture of polymers (polyallyl resin and polyurethane) and a topmost water-soluble PVA layer. The PVA layer is washed away with water before printing (see the Fabrication section for details), thus ending with a three-layered tattoo paper structure. Notably, the tattoo decal film adopted here has a transfer layer made of polyurethane/allyl resin film with a thickness of 1.5 µm. This substrate has been shown to improve the mechanical stability of TTEs on skin with respect to the ~500 nm thick ethyl cellulose-based tattoo decal paper previously used[22]. The glue part is also a three-layered sheet composed of a silicone carrier sheet, an acrylic glue (thickness ≈ 700 nm) and a plastic liner. The glue part was used for providing tattoo adhesion while preventing the direct contact of interconnection lines with skin. Polyethylene naphthalene (PEN, by Goodfellow, thickness 1.3 µm) was employed as a substrate for flat connector and Polyimide tape (Kapton tape by 3 M, thickness 50 µm) for back support of the external part of the connection.

Fabrication

The fabrication process included inkjet printing of electrodes, interconnections, and assembling of the flat contact through a lamination process. Inkjet printing is carried out with a Dimatix DMP-2800 system (Fujifilm Corp., Japan) with a 10 pL cartridge (DMC-11610). PEDOT:PSS ink is used after filtration (Minisart, average pore size 0.20 µm, Sartorius). Electrodes are prepared in three steps: the temporary tattoo paper washing, the electrodes printing and the lamination process for the TTE's assembly. The tattoo paper was attached on a flat and rigid support (an acrylic transparent sheet, thickness 3 mm) with a tape, to avoid any water infiltration on the backside. Then, the surface is washed with DI water until the PVA layer is completely removed; the tattoo paper visibly changes its wettability. Finally, the tattoo paper is dried with compressed air. PEDOT:PSS is then ink-jet printed according to a customized electrodes design onto the washed tattoo paper (sensitive area diameter = 12 mm) while a line (width = 3 mm, length = 12 mm) is printed onto a rectangular PEN substrate (width = 8 mm, length = 12 mm) in order to produce the external interconnection. The printing process is carried out by jetting through three adjacent nozzles at 5 kHz; drop spacing is set at 20 µm. Such parameters are optimized to minimize coffee ring effect and to obtain a consistent printing. In order to achieve low resistance electrodes, both the sensor and the connection are produced via multiple layer printing. In the case of electrodes printed onto temporary tattoo paper, after each layer was printed the tattoo was annealed in a convection oven at 110 °C, for 10 min. For the external interconnection three subsequent PEDOT:PSS layers are deposited with a final drying step in a convection oven at 110 °C for 15 min. Finally, the assembly of TTE is carried out by lamination of various components. The glue sheet, from the tattoo kit, is patterned with a hole in the top part (diameter = 11.3 mm), corresponding to the sensitive area of the printed tattoo electrode (1 cm^2). The external interconnection supported by PEN is laminated onto the printed tattoo. The glue sheet is added on top with a piece of Kapton tape and placed on the end part of the PEN. The glue layer included a plastic liner to be removed by peeling prior to transfer of the assembled TTE on the skin. Assembled electrodes are transferred onto skin by gently pressing the tattoo against the skin and wetting the supporting paper, which caused the dissolution of the sacrificial PVA layer. The clip-like homemade connector is 3D printed (Ultimaker) from ABS material and connects the TTE to a standard recording cable. The inner parts of the clip are metallized and soldered to the cable.

Impedance assessment

The impedance evaluation is performed with an Autolab potentiostat (Metrohm Autolab B.V.). The measurements are executed in three electrodes configuration, with 2.5 cm center-to-center interspace between them. The counter (CE) and the Working (WE) electrodes are Ag/AgCl electrodes (by Ambu BlueSensor, REF M-00-S/50), while the electrode of interest in each measurement, TTEs or Ag/AgCl, acted as the Working Electrode (WE). All the impedance measurements are performed on the forearm with 1 cm^2 electrodes. The measurements are done in potentiometric mode with an applied sinusoidal signal of 1 mV amplitude. The frequency range is set between 0.1 Hz and 0.1 MHz.

Phantom platform

The phantom evaluation platform was fabricated from pure powdered agarose (Thermo Fisher Scientific, New Jersey, USA) as described in the literature[64]. A saline solution is prepared by adding 15 mg/ml NaCl (99.8% purity Sigma St. Louis, Missouri, USA) to deionized ultra-filtered water at 85–90 °C. Agarose powder is then added to achieve the desired gel concentration (1.2% by weight). The solution is stirred with a magnetic bar in a rectangular glassware and then cooled at room temperature. The agarose solid block is then combined with a prefabricated board of planar electrodes as an on skin-mimicking platform. The board is made of four Cu electrodes (1 cm^2 area, 2 cm inter-electrodes distance) in line. It is aimed to send bipolar signals of different amplitudes from the bottom of the phantom simulating simultaneous electrophysiological events. On the top of the phantom two kind of electrodes are positioned: Ag/AgCl (by Ambu BlueSensor, REF M-00-S/50) and TTEs. The signal is recorded in a bipolar way from two couple of top electrodes. The sent signals and the recordings are administrated and then processed with a dedicated LabView program

through a National Instrument Data acquisition device (NI myDAQ). The sent signal is composed of two profiles: the first (defined as the square wave in the text) with an amplitude of 1 V and a frequency of 50 Hz, and the second (denominated as the peak in the text) with an amplitude of 2 V and a frequency of 5 Hz. The square wave is sent between the left couple of the electrodes, while the peak is sent through the couple of electrodes on the right. All the recordings are done at ambient conditions.

EEG/MEG evaluations

TTEs were placed in T7, Cz, Oz, Fp1, and Fp2 locations according to the 10–20 positioning system[65]. We used the Cz-Oz derivation for the detection of alpha waves and the T7-Oz for the recording of the AEP. In order to compare the signal acquisition during the AEP test, two Ag/AgCl electrodes (disposable adhesive disks by Technomed, 20 mm overall diameter, 1 cm^2 sensing area) are placed in an adjacent position, named sT7-sOz. A TTE reference is placed on the right mastoid bone, while the TTE ground is located at the highest point of the head, near the Cz position. The EEG recordings are obtained using a multichannel bipolar amplifier (BrainAmp ExG MR 16, BrainProducts) allowing simultaneous recordings with different types of electrodes. For alpha waves evaluations, spontaneous recordings are performed on a comfortably seated participant in an isolated room. The participant is asked to close his eyes in order to develop alpha wave for a period of 2 min and subsequently to open his eyes to stop their appearance. AEPs are obtained with a pure tone of 750 Hz of 30 ms duration (0.3 ms rise and decay) delivered through ear plugs (Stax SRM-727II amplifier and Etymotic ear insert R13-14) at comfortable level with an inter-stimulus interval of 400–600 ms and repeated 550 times. The signal is recorded with a band-pass filter 0.016–1000 Hz, at a sampling rate of 2500 Hz.

MEG recordings are performed in a MEG room with a 4D whole head Neuroimaging system (WH3600™), with a band pass of DC-800Hz and a sampling rate of 2134.51 Hz. The participant is lying on a special head-holding bed placed under MEG sensors.

Post-acquisition signal processing

All recordings are reviewed and digitally filtered using a 3–40 Hz band pass filter with the Anywave software[66]. The data are then analysed using custom-written tools from the Fieldtriep MATLAB (Mathworks) toolbox[67].

Experiments involving human participants

Two able-bodied participants (one male and one female aged 33.5 ± 3.5 years old) free of any motor and neural disorders gave their informed consent and participated in this study. One participant performed the impedance recordings with the three diverse TTEs sets while another participant volunteered in the EEG/MEG evaluations with TTEs and Ag/AgCl electrodes. All experiments are performed following Timone hospital's regulations regarding personal data protection. The experiment was conducted under conditions provided for by French regulations.

Reporting summary

Further information on research design is available in the Nature Research Reporting Summary linked to this article.

DATA AVAILABILITY

The experimental data referenced in this text is available from the authors upon reasonable request.

Received: 17 October 2019; Accepted: 20 February 2020;
Published online: 17 March 2020

REFERENCES

1. Berger, H. Über das elektrenkephalogramm des menschen. *Eur. Arch. Psychiatry Clin. Neurosci.* **87**, 527–570 (1929).
2. Teplan, M. Fundamentals of EEG measurement. *Meas. Sci. Rev.* **2**, 1–11 (2002).
3. Pfurtscheller, G. & Aranibar, A. Evaluation of event-related desynchronization (ERD) preceding and following voluntary self-paced movement. *Electroencephalogr. Clin. Neurophysiol.* **46**, 138–146 (1979).
4. Tadel, F., Baillet, S., Mosher, J. C., Pantazis, D. & Leahy, R. M. Brainstorm: a user-friendly application for MEG/EEG analysis. *Comput. Intell. Neurosci.* **2011**, 8 (2011).
5. Wijdicks, E. F. M. Determining brain death in adults. *Neurology* **45**, 1003–1011 (1995).
6. Dauwels, J., Vialatte, F., Musha, T. & Cichocki, A. A comparative study of synchrony measures for the early diagnosis of Alzheimer's disease based on EEG. *NeuroImage* **49**, 668–693 (2010).
7. Gavaret, M. et al. Source localization of scalp EEG interictal spikes in posterior cortex epilepsies investigated by HR EEG and SEEG. *Epilepsia* **50**, 276–289 (2009).
8. Müller-Putz, G. R. et al. The future in brain/neural computer interaction: Horizon 2020. p 48 (Graz: EU & Graz University of Techology, 2015).
9. Tallgren, P., Vanhatalo, S., Kaila, K. & Voipio, J. Evaluation of commercially available electrodes and gels for recording of slow EEG potentials. *Clin. Neurophysiol.* **116**, 799–806 (2005).
10. Ferree, T. C., Luu, P., Russell, G. S. & Tucker, D. M. Scalp electrode impedance, infection risk, and EEG data quality. *Clin. Neurophysiol.* **112**, 536–544 (2001).
11. Nunez, P. L. & Srinivasan, R. *Electric Fields of the Brain: The Neurophysics of EEG*. (Oxford University Press, Oxford, 2006).
12. Lantz, G., De Peralta, R. G., Spinelli, L., Seeck, M. & Michel, C. M. Epileptic source localization with high density EEG: how many electrodes are needed? *Clin. Neurophysiol.* **114**, 63–69 (2003).
13. Chi, Y. M., Jung, T.-P. & Cauwenberghs, G. Dry-contact and noncontact biopotential electrodes: methodological review. *IEEE Rev. Biomed. Eng.* **3**, 106–119 (2010).
14. Searle, A. & Kirkup, L. A direct comparison of wet, dry and insulating bioelectric recording electrodes. *Physiol. Meas.* **21**, 271 (2000).
15. Fiedler, P. et al. in *XII Mediterranean Conference on Medical and Biological Engineering and Computing 2010*. 418–421 (Springer, 2010).
16. Xing, X. et al. A high-speed SSVEP-based BCI using dry EEG electrodes. *Sci. Rep.* **8**, 14708 (2018).
17. Stauffer, F. et al. Skin conformal polymer electrodes for clinical ECG and EEG recordings. *Adv. Healthc. Mater.* **7**, 1700994 (2018).
18. Nawrocki, R. A. et al. Self adhesive and ultra conformable, Sub 300 nm dry thinfilm electrodes for surface monitoring of biopotentials. *Adv. Funct. Mater.* **28**, 1803279 (2018).
19. Tian, L. et al. Large-area MRI-compatible epidermal electronic interfaces for prosthetic control and cognitive monitoring. *Nat. Biomed. Eng.* **3**, 194 (2019).
20. Kabiri Ameri, S. et al. Graphene electronic tattoo sensors. *ACS Nano* **11**, 7634–7641 (2017).
21. Zucca, A. et al. Tattoo conductive polymer nanosheets for skin-contact applications. *Adv. Healthc. Mater.* **4**, 983–990 (2015).
22. Ferrari, L. M. et al. Ultraconformable temporary tattoo electrodes for electrophysiology. *Adv. Sci* **5**, 1700771 (2018).
23. da Silva, F. L. EEG and MEG: relevance to neuroscience. *Neuron* **80**, 1112–1128 (2013).
24. Bandodkar, A. J., Jia, W. & Wang, J. Tattoo based wearable electrochemical devices: a review. *Electroanalysis* **27**, 562–572 (2015).
25. Kim, D. H. et al. Epidermal electronics. *Science* **333**, 838–843 (2011).
26. Jia, W. et al. Electrochemical tattoo biosensors for real-time noninvasive lactate monitoring in human perspiration. *Anal. Chem.* **85**, 6553–6560 (2013).
27. Bareket, L. et al. Temporary-tattoo for long-term high fidelity biopotential recordings. *Sci. Rep.* **6**, 25727 (2016).
28. Liu, Y., Pharr, M. & Salvatore, G. A. Lab-on-skin: a review of flexible and stretchable electronics for wearable health monitoring. *ACS Nano* **11**, 9614–9635 (2017).
29. Chapman, B. N. Thin-film adhesion. *J. Vac. Sci. Technol.* **11**, 106–113 (1974).
30. Barsotti, J. et al. Ultraconformable freestanding capacitors based on ultrathin polyvinyl formal films. *Adv. Electron. Mater* **4**, 1800215 (2018).
31. Mehrali, M. et al. Blending electronics with the human body: a pathway toward a cybernetic future. *Adv. Sci* **5**, 1700931 (2018).
32. Sekitani, T. & Someya, T. Stretchable, large-area organic electronics. *Adv. Mater.* **22**, 2228–2246 (2010).
33. Jeong, J. W. et al. Soft materials in neuroengineering for hard problems in neuroscience. *Neuron* **86**, 175–186 (2015).
34. Bihar, E. et al. Fully printed electrodes on stretchable textiles for long-term electrophysiology. *Adv. Mater. Technol.* **2**, 1600251 (2017).
35. Takamatsu, S. et al. Direct patterning of organic conductors on knitted textiles for long-term electrocardiography. *Sci. Rep.* **5**, 15003 (2015).
36. Leleux, P. et al. Conducting polymer electrodes for electroencephalography. *Adv. Healthc. Mater.* **3**, 490–493 (2014).
37. Arias, A. C., MacKenzie, J. D., McCulloch, I., Rivnay, J. & Salleo, A. Materials and applications for large area electronics: solution-based approaches. *Chem. Rev.* **110**(1), 3–24 (2010).

38. Kappenman, E. S. & Luck, S. J. The effects of electrode impedance on data quality and statistical significance in ERP recordings. *Psychophysiology* **47**, 888–904 (2010).
39. Cole, K. S. In *Cold Spring Harbor Symposia on Quantitative Biology*. 110–122 (Cold Spring Harbor Laboratory Press, 2018).
40. Yamamoto, T. & Yamamoto, Y. Electrical properties of the epidermal stratum corneum. *Med. Biol. Eng.* **14**, 151–158 (1976).
41. Lukacs, Z. The numerical evaluation of the distortion of EIS data due to the distribution of parameters. *J. Electroanal. Chem.* **432**, 79–83 (1997).
42. Geddes, L. A. & Baker, L. E. The specific resistance of biological material—a compendium of data for the biomedical engineer and physiologist. *Med. Biol. Eng.* **5**, 271–293 (1967).
43. Neuman, M. R. Biomedical Sensors. In *Wiley Encyclopedia of Electrical and Electronics Engineering* (ed. Webster, J. G.) (1999).
44. Alanen, E., Nuutinen, J., Nicklén, K., Lahtinen, T. & Mönkkönen, J. Measurement of hydration in the stratum corneum with the MoistureMeter and comparison with the Corneometer. *Ski. Res. Technol.* **10**, 32–37 (2004).
45. Corcuff, P., Bertrand, C. & Leveque, J. L. Morphometry of human epidermis in vivo by real-time confocal microscopy. *Arch. Dermatol. Res.* **285**, 475–481 (1993).
46. Reilly, J. P. Applied Bioelectricity: From Electrical Stimulation to Electropathology (Springer, 2012).
47. Gabriel, C. *Compilation of the Dielectric Properties of Body Tissues at RF and Microwave Frequencies* (King's College London, 1996).
48. Björklund, S. et al. Skin membrane electrical impedance properties under the influence of a varying water gradient. *Biophys. J.* **104**, 2639–2650 (2013).
49. Peng, H.-L. et al. Parylene-based flexible dry electrode for bioptential recording. *Sens. Actuators B* **231**, 1–11 (2016).
50. Hooge, F. N., Kleinpenning, T. G. M. & Vandamme, L. K. J. Experimental studies on 1/f noise. *Rep. Prog. Phys.* **44**, 479 (1981).
51. Gilden, D. L., Thornton, T. & Mallon, M. W. 1/f noise in human cognition. *Science* **267**, 1837 (1995).
52. Voytek, B. et al. Age-related changes in 1/f neural electrophysiological noise. *J. Neurosci.* **35**, 13257–13265 (2015).
53. Hillyard, S. A., Hink, R. F., Schwent, V. L. & Picton, T. W. Electrical signs of selective attention in the human brain. *Science* **182**, 177–180 (1973).
54. Rosburg, T., Boutros, N. N. & Ford, J. M. Reduced auditory evoked potential component N100 in schizophrenia—a critical review. *Psychiatry Res.* **161**, 259–274 (2008).
55. Puce, A. & Hämäläinen, M. A review of issues related to data acquisition and analysis in EEG/MEG studies. *Brain Sci.* **7**, 58 (2017).
56. Hansen, P., Kringelbach, M. & Salmelin, R. *MEG: An Introduction to Methods* (Oxford University Press, 2010).
57. Badier, J. M. et al. Technical solutions for simultaneous MEG and SEEG recordings: towards routine clinical use. *Physiol. Meas.* **38**, N118 (2017).
58. Chu, C. J. High density EEG—What do we have to lose? *Clin. Neurophysiol.* **126**, 433–434 (2015).
59. Fender, D. H. Source localization of brain electrical activity. *Handb. Electroencephalogr. Clin. Neurophysiol.* **1**, 355–403 (1987).
60. Lantz, G., Grouiller, F., Spinelli, L., Seeck, M. & Vulliemoz, S. Localisation of focal epileptic activity in children using high density EEG source imaging. *Epileptologie* **28**, 84–90 (2011).
61. Srinivasan, R., Tucker, D. M. & Murias, M. Estimating the spatial Nyquist of the human EEG. *Behav. Res. Methods Instrum. Comput.* **30**, 8–19 (1998).
62. Dabek, J. et al. Determination of head conductivity frequency response in vivo with optimized EIT-EEG. *NeuroImage* **127**, 484–495 (2016).
63. Gevins, A. et al. High resolution EEG: 124-channel recording, spatial deblurring and MRI integration methods. *Electroencephalogr. Clin. Neurophysiol.* **90**, 337–358 (1994).
64. Kandadai, M. A., Raymond, J. L. & Shaw, G. J. Comparison of electrical conductivities of various brain phantom gels: developing a 'brain gel model'. *Mater. Sci. Eng.* **32**, 2664–2667 (2012).
65. Jasper, H. Report of the committee on methods of clinical examination in electroencephalography. *Electroencephalogr. Clin. Neurophysiol.* **10**, 370–375 (1958).
66. Colombet, B., Woodman, M., Badier, J. M. & Bénar, C. G. AnyWave: a cross-platform and modular software for visualizing and processing electrophysiological signals. *J. Neurosci. Methods* **242**, 118–126 (2015).
67. Oostenveld, R., Fries, P., Maris, E. & Schoffelen, J.-M. FieldTrip: open source software for advanced analysis of MEG, EEG, and invasive electrophysiological data. *Comput. Intell. Neurosci.* **2011**, 1687–5265 (2011).

ACKNOWLEDGEMENTS

The authors want to thank Michel Fiocchi for his help with the phantom platform development. This work was supported by BPI France AUTONOTEX project, an ANR JCJC OrgTex project, and by French Life Imaging (FLI). F.G. acknowledges financial support from Top Global University Program at Waseda University, Tokyo from MEXT Japan. We would like to thank Simon Regal, a master student fellow, for his contribution in preliminary evaluations of tattoo electrodes. E.I. wishes to thank CMP cleanroom staff for their technical support during the development of the project.

AUTHOR CONTRIBUTIONS

F.G. and E.I. conceived the study. F.G. and L.M.F. previously developed tattoo fabrication strategy. L.M.F. and U.I. made the experimental work, supervised by E.I. J.M.B. performed the EEG/MEG recordings, with L.M.F., U.I. and E.I. L.M.F., E.I., and F.G. prepared the manuscript and figures.

COMPETING INTERESTS

The authors declare no competing interests.

ADDITIONAL INFORMATION

Supplementary information is available for this paper at https://doi.org/10.1038/s41528-020-0067-z.

Correspondence and requests for materials should be addressed to F.G. or E.I.

Reprints and permission information is available at http://www.nature.com/reprints

Publisher's note Springer Nature remains neutral with regard to jurisdictional claims in published maps and institutional affiliations.